

High-frequency powers hidden within QRS complex as an additional predictor of lethal ventricular arrhythmias to ventricular late potential in post-myocardial infarction patients

Takeshi Tsutsumi, MD,* Nami Takano, MD,[†] Narihisa Matsuyama, MD,[‡] Yukei Higashi, MD,[§] Kuniaki Iwasawa, MD,[¶] Toshiaki Nakajima, MD[†]

From the *Division of Cardiology, Eda Memorial Hospital, Yokohama, Japan, [†]Department of Ischemic Circulatory Physiology, University of Tokyo, Tokyo, Japan, [‡]Yamamoto Clinic, Kanagawa, Japan, [§]Division of Cardiology, Showa University Fujigaoka Hospital, Yokohama, Japan, [¶]Division of Health Service Promotion, University of Tokyo, Tokyo, Japan.

BACKGROUND Ventricular late potentials (VLPs) have been known to be a predictor of lethal ventricular arrhythmias (L-VAs); however, detection of other arrhythmogenic signals within the QRS complex remains obscure.

OBJECTIVE The aim of this study was to evaluate whether abnormal intra-QRS high-frequency powers (IQHFP) within the QRS complex become a new predictor of L-VAs in addition to VLPs.

METHODS Both 12-lead electrocardiograms (ECG) and VLPs were recorded from 142 subjects, including 37 patients without heart diseases, 97 patients post-myocardial infarction (MI), and 45 post-MI patients with L-VAs. Time-frequency analysis of ECG (leads V₁ or II) using wavelet transform with the Morlet function was performed. After the time-frequency powers were calculated, the ratios of the peak of signal power during the QRS complex in high-frequency bands against the peak power at 80 Hz (b/a ratio; P100, P150, P200, P250, or P300Hz/P80Hz) were measured. Abnormal IQHFP was defined when the b/a ratio exceeded the optimal cut-off values estimated by receiver-operator characteristic curves.

RESULTS The combination of abnormal IQHFP appearing at 200, 250, and 300 Hz with positive VLPs increased the sensitivity for prediction of L-VAs from 53.3% by VLPs to 89.5%, and the negative predictive value from 74.7% by VLPs to 87.7%.

CONCLUSION The combined use of VLPs and IQHFP hidden within the QRS complex improved the prediction of L-VAs in post-MI patients.

KEYWORDS Lethal ventricular arrhythmias; Wavelet transform; Intra-QRS arrhythmogenic signals; Ventricular late potential

ABBREVIATIONS AIQP = abnormal intra-QRS potential; CWT = continuous wavelet transform; fQRS = fragmented QRS; IQHFP = intra-QRS high-frequency powers; L-VAs = lethal ventricular arrhythmias; MI = myocardial infarction; ROC = receiver-operator characteristic; SAECG = signal-averaged electrocardiogram; SCD = sudden cardiac death; VF = ventricular fibrillation; VLP = ventricular late potential; VT = ventricular tachycardia; WT-ECG = wavelet transformed electrocardiographic

(Heart Rhythm 2011;8:1509–1515) © 2011 Heart Rhythm Society. All rights reserved.

Introduction

Despite recent advances in available therapies, pre-existing ischemic heart disease is manifested in 80% of victims of sudden cardiac death (SCD).¹ Lethal ventricular arrhythmias (L-VAs), such as ventricular tachycardia (VT) and ventricular fibrillation (VF), were responsible for the events culminating in SCD. To date, noninvasive markers of SCD used in clinical practice for detecting depolarization abnormalities in the heart include: (1) ventricular late potential (VLP) on signal-averaged electrocardiogram (SAECG),^{2,3} (2) abnormal intra-QRS potentials (AIQPs),⁴ (3) fragmented QRS (fQRS),⁵ and (4) repolarization abnormalities.⁶ Re-

cently, Bauer et al demonstrated that the presence of VLPs in post-myocardial infarction (MI) patients in the reperfusion era was of little value for predicting L-VAs.⁷ The intramural fragmented activities, presumed to be the source of VLPs, were not only generated at the phase of the terminal QRS complex but also at the other phases of QRS in the experimental study.⁸ Therefore, tentative studies of spectral turbulence analysis,⁹ spectral mapping,¹⁰ AIQPs, and time-frequency analysis using wavelet transform^{11–13} have been performed to detect abnormal electrical signals within the QRS in addition to VLPs. However, with the exception of VLPs, additional methods have not been fully established in routine clinical applications. Further reliable studies should be devised. In the present study, time-frequency analysis of a single QRS complex applying wavelet transform was performed. We noted that abnormal wavelet transformed electrocardiograms signals (WT-ECG signals),

Address reprint requests and correspondence: Dr. Takeshi Tsutsumi, Division of Cardiology, Eda Memorial Hospital, 1-1 Azamino Minami, Aoba-Ku, Yokohama, 225-0012, Japan. E-mail address: tsutsumi07@gmail.com. (Received March 16, 2011; accepted June 24, 2011)

which appeared at high-frequency bands (200 to 300 Hz) observed within the QRS complex (intra-QRS high-frequency power; IQHFP), were frequently seen in post-MI patients with L-VAs. It was assumed that abnormal IQHFP originates from the invisible arrhythmogenic potentials within the QRS complex. The aim of this study was to demonstrate that the recognition of abnormal IQHFP within the QRS complex could enhance the prediction of VLPs for L-VAs in post-MI patients.

Methods

Subjects and electrocardiographic data acquisition

Five hundred and seventy-six patients admitted to the Showa University Fujigaoka Hospital from 2004 to 2009 underwent examination to detect VLPs for prediction of L-VAs. The subjects of this study comprised 142 consecutive patients with MI in Table 1 and age-matched 37 patients without heart diseases (normal subjects). Each patient was transported by ambulance to the hospital, diagnosed with acute MI or post-MI unstable angina, and underwent

Table 1 Characteristics of patients with myocardial infarction

	Myocardial infarction		P value
	MI without L-VAs	MI with L-VAs	
Number of cases	97	45	
Age (yrs)	68.5 ± 11.7	66.2 ± 11.5	.272
Sex (M/F)	77/20	41/4	.083
MI (Ant/Inf)	58/39	34/11	.067
CTR (%)	55.6 ± 6.5	53.6 ± 5.4	.514
EF (%)	46.5 ± 11.4	40.5 ± 9.1	.512
Peak CK (IU/L)	2,874 ± 2,126	5,041 ± 4,879	.058
CK-MB(IU/L)	267 ± 209	336 ± 284	.356
SVD	48 (48.4%)	23 (51.0%)	.858
DVD	24 (24.7%)	9 (20.0%)	.534
TVD	19 (19.6%)	13 (28.9%)	.212
CABG	12 (12.4%)	3 (6.7%)	.303
Inducible VT	0%	18 (40.0%)	
ICD	0%	13 (28.8%)	
Time of recording VLP			
1st attack	71 (73.1%)	19 (42.5%)	<.001
2nd and 3rd attacks	33 (33.0%)	29 (64.4%)	<.001
Medication			
Amiodarone	0%	28 (62.2%)	
Na channel B	0%	7 (15.5%)	
β-blocker	41 (42.3%)	6 (13.3%)	<.001
No antiarrhythmic drug	56 (57.7%)	12 (26.7%)	<.05

Normal ranges of creatine kinase (CK) and CK-MB are 57 to 197 IU/L and 25 IU/L or less.

Ant = anterior myocardial infarction; CABG = coronary artery bypass grafting; peak CK = peak value of serum creatine kinase; CTR = cardiothoracic ratio; DVD = double-vessel disease; EF = ejection fraction; F = female; Na channel B = sodium channel blocker; M = male; ICD = implantable cardioverter defibrillator; Inf = inferior myocardial infarction; L-VAs = lethal ventricular arrhythmias; MI = myocardial infarction; SVD = single-vessel disease; TVD = triple-vessel disease; VLP = ventricular late potential; VT = ventricular tachycardia.

urgent percutaneous coronary intervention. The diagnosis of MI was confirmed by characteristic ST-segment changes and enzymatic assessment (peak value of serum creatine kinase [peak CK] and CK-MB) in the acute phase, and thallium-201 imaging in the chronic phase. The characteristics of the severity of MI including average peak CK, CK-MB, and number of coronary arteries with significant stenosis are summarized in Table 1.

SAECG and standard 12-lead electrocardiogram (ECG) were recorded at the same time. Ninety of the patients with MI underwent both examinations within 1 month after the heart attack, and the remaining 52 patients underwent these examinations during the chronic phase of MI. The following cases were excluded in this study: Wolff-Parkinson-White syndrome, implanted pacemaker or after implantable cardioverter-defibrillator, pre-existing bundle branch blocks, intraventricular conduction block, and persistent atrial fibrillation. These cases comprised 9.6% of all subjects. The 45 post-MI patients with symptomatic L-VAs during the clinical course or with L-VAs induced by programmed ventricular stimulation were selected for this study. The standard programmed stimulation method was applied to the induction of VT or VF. If sustained VT for at least 10 seconds with cycle length of 200 ms or more was induced by 3 extrastimuli, the result was considered positive. Both SAECG and ECG were recorded within 1 to 3 days before the electrophysiological study. The normal group consisted of the patients without detectable heart diseases in ECG, chest X-ray film, and echocardiogram, and of healthy volunteers (n = 37: male: 45.9%, female: 54.1%, age: 53.5 ± 14.9 years). The ethical committee of Showa University Fujigaoka Hospital approved the protocol of this study.

A device (Cardio-Multi, FDX-6521; Fukuda Densi, Co. Ltd., Tokyo, Japan) was used to record both SAECG and ECG in the shield room. Bipolar pseudo-orthogonal X, Y, and Z leads were used to measure VLPs, with frequency cut-off between 40 and 250 Hz. Approximately 200 beats were filtered and averaged. Three variables of SAECG are considered to assess the presence of VLPs: (1) a QRS duration of 114 ms or more, (2) a duration of the low-amplitude signal <40 μV in the terminal portion of the averaged QRS complex of 38 ms or more, (3) a root mean square of the terminal 40 ms of the filtered QRS of 20 μV or less. VLPs were present when at least 2 of these showed abnormal values.³ Based on these findings, true-positive VLP patients were defined as the post-MI patients who had both positive VLPs and an episode of spontaneous or inducible L-VAs. Post-MI patients were classified into 4 groups: (1) true-positive VLPs (n = 24), (2) false-negative VLPs (n = 21), (3) false-positive VLPs (n = 35), (4) true-negative VLPs (n = 62). After measuring VLPs, ECGs were recorded for 20 seconds through a 300-Hz Butterworth high-cut filter and digitized using a 16-channel A/D converter with 16-bit resolution, at a sampling rate of 10 kHz.

Time-frequency analysis

The continuous wavelet transform (CWT) was applied to the time-frequency analysis of the ECG signal. The time-frequency powers using CWT were calculated using a method reported in previous studies.^{12,13} In the present study, commercial PC software developed by our group (BIOMAS for Wavelet, version 3.0, Elmec Co. Ltd., Tokyo, Japan) was used to measure WT-ECG signals. The time-frequency powers during QRS complex in a range from 5 to 300 Hz were calculated by CWT with 40 scale bands. The Morlet function was applied to measure WT-ECG signals in this study because it was fitted to analyze the target frequency of this study. In contrast, if the Gabor function was applied, the oscillatory CWT-ECG signals similar to the chirp oscillation were mixed at high-frequency ranges, which might be related to the width of the original mother wavelet in this software.

To avoid incorporation into artifacts, P-QRS-T waves without visual baseline drift or noises were selected from continuous records of ECG for 20 seconds. In cases of anterior or anterolateral MI, a single QRS complex in chest leads (V_1 or V_2) was analyzed, and in cases of inferior or posterolateral MI, that in a limb lead (II or III) was analyzed. Subsequently, the transformed data were displayed on the computer screen as 80 lines of WT-ECG signals that were represented every 4.19 Hz, ranged from 5 to 350 Hz.

Measurements of wavelet-transformed signals and exclusion criteria to avoid error

WT-ECG signals given from 2 frequency scale bands (80 and 300 Hz) were optionally selected and displayed as a function of time in Figure 1. As shown in Figure 1A, the major frequency powers were observed within the QRS

complex whose peak amplitudes indicated by dotted lines (a, b) appeared at the early descending limb of the QRS complex. The ratio of the peak signal amplitude (b/a ratio) was 0.15 in this case. The use of this method of displaying a pair of wavelet signals made it possible to distinguish the fine wavelet signals from the noise. In addition, the following exclusion criteria empirically arranged: (1) the **a** value was within average normal values ± 1 SD ($0.17 >$, or $>0.06 \text{ mv}^2/\text{Hz}$), (2) the **b** value was larger by at least 2-fold power than the powers derived from noise between the U-P segment where the electrical generator in the heart was null. If the **a** value was $0.06 \text{ mv}^2/\text{Hz}$ or less, the noise signals were sometimes magnified. By adopting these exclusion criteria, 8.5% of the total subjects were eliminated from the study. In Figure 1B, a magnified picture at the foot of WT-ECG signals and ECG are shown. The duration of the WT-ECG signal corresponding to the IQHFP was 36.0 ms in this case.

Statistical analysis

Data are expressed as the mean ± 1 SD. A paired-sample *t* test was used for comparison of continuous variables between the 2 study groups. The χ^2 test with Yates correction for 2×2 tables was used to compare the categorical data. For multiple-group comparisons, statistical significance was assessed by analysis of variance, followed by the Tukey Honestly Significant Difference Adjustment for multiple comparisons. To get an appropriate sensitivity and specificity, receiver-operator characteristics (ROC) curves were used to optimize the cut-off values of b/a ratios in each high-frequency band (300, 250, 200, and 150 Hz). The optimum parameters associated with ROC curves were given from the shortest distance from the upper and left

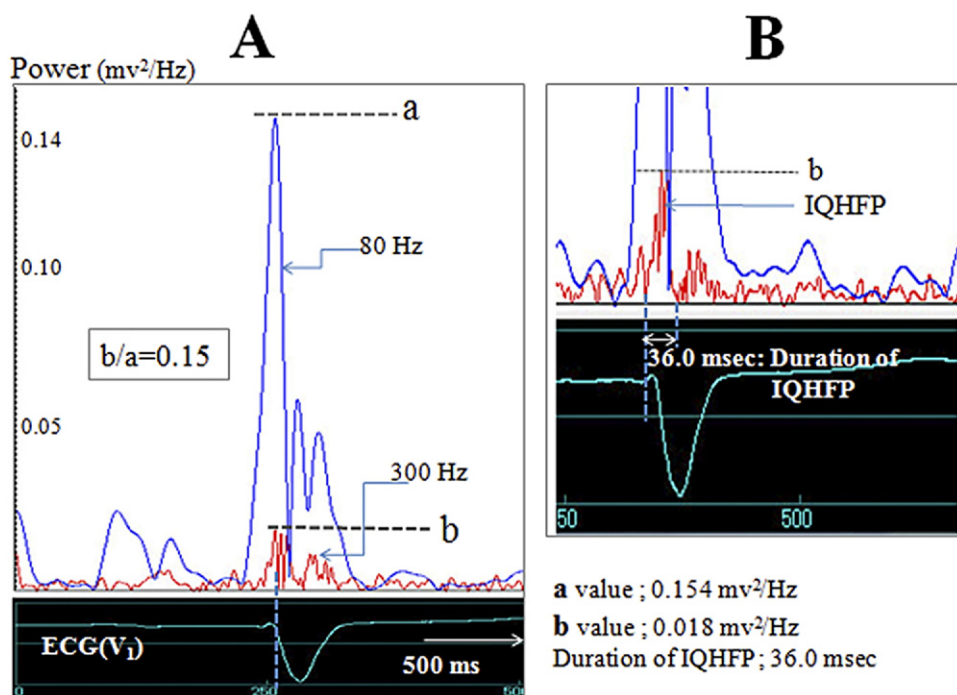


Figure 1 Methods for measurement of parameters from wavelet-transformed ECG signals. **A:** The chest ECG was recorded from a 56-year-old male patient with anterior infarction without lethal ventricular arrhythmias. The blue lines indicate WT-ECG signals at 80 Hz. The red lines indicate WT-ECG signals at 300 Hz. WT-ECG signals correspond to the time course of ECG. The letters **a** and **b** indicate the peak frequency power of WT-ECG signal at 80 Hz or 300 Hz within the QRS complex, respectively. **B:** A magnified picture at the foot of wavelet-transformed signals and ECG are shown. ECG = electrocardiogram; IQHFP = intra-QRS high-frequency power; WT-ECG = wavelet-transformed electrocardiogram.

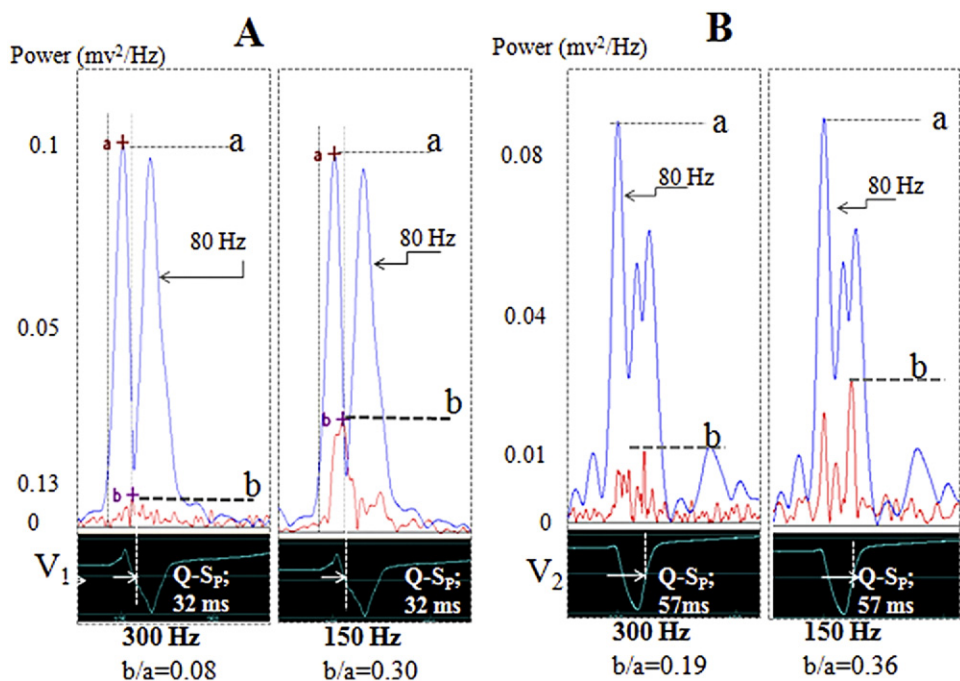


Figure 2 Frequency-dependent changes in high-frequency power in a normal subject and in a patient post-myocardial infarction. Two selective WT-ECG signals corresponding to the time course of ECG (V₁ or V₂) from a normal subject (A) and a patient with myocardial infarction with lethal ventricular arrhythmia (B) are illustrated. In each panel, blue lines indicate WT-ECG signals at 80 Hz, and red lines indicate WT-ECG signals at 300 and 150 Hz. ECG = electrocardiogram; Q-S_p = appearance time of the peak wavelet signal from the onset of the QRS complex at 150 Hz and 300 Hz; WT-ECG = wavelet-transformed electrocardiogram.

corner (sensitivity = 1.0) of the graph to the ROC curve. A value of *P* < .05 was considered statistically significant.

Results

b/a ratio in each group

In Figure 2, WT-ECG signals from a normal subject (Figure 2A) and an MI patient with L-VAs (Figure 2B) are shown. The b/a ratio at 300 Hz was obviously smaller in a normal subject compared with an MI patient. The peak powers of the high-frequency signals within the QRS complex indicate that **b** appearing at the descending limb of the QRS whose time of appearance was 32 ms after the onset of QRS (Q-S_p time in the figure) in normal subjects. The peak power of the WT-ECG signals traced by red lines increased as the frequency was lowered. Consequently, b/a ratios were increased from 300 to 150 Hz, and their values were 0.08 at 300 Hz, and 0.30 at 150 Hz. In Figure 2B, 2 selective WT-ECG signals calculated from the ECG (V₂) of a patient with MI and L-VAs are shown. Multiple peaks were observed, especially at 300 Hz, at the early and the late phases

of the QRS complex as compared with the normal subject shown in Figure 2A. The peak powers of the signals appeared at the late phase of QRS, indicated by **b**, that appeared at 57 ms after the onset of QRS. In addition, b/a ratios in both frequency bands were greater than those in the normal subject.

Averaged intra-QRS high-frequency potentials (b/a ratio) in all groups

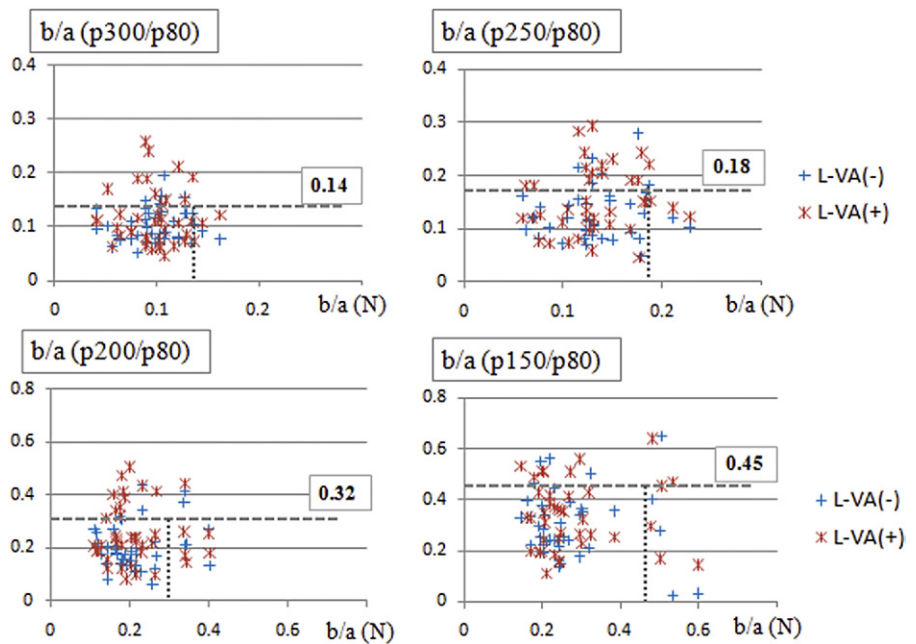
After the time-frequency powers were calculated, the ratios of the peak of signal power during the QRS complex in high-frequency bands against the peak power at 80 Hz (b/a ratio; P100, P150, P200, P250, or P300Hz/P80Hz) were measured. The mean values of b/a ratios in every group are shown in Table 2. The post-MI patients were divided into 4 groups based on whether VLPs were positive or negative. Significant differences in b/a ratios were found between the group of false-negative VLPs and normal subjects at 300, 250, and 150 Hz (*P* < .05). The b/a ratios at 250 and 200 Hz were higher in false-negative VLPs compared with those in

Table 2 The b/a ratios in each group

Groups	b/a ratio (mean ± SD)				
	P300/P80 Hz	P250/P80 Hz	P200/P80 Hz	P150/P80 Hz	P100/P80 Hz
Normal objects (n = 37)	0.098 ± 0.028*	0.136 ± 0.048*	0.213 ± 0.114	0.278 ± 0.114*	0.626 ± 0.130
MI without VA	0.102 ± 0.031	0.131 ± 0.052†	0.205 ± 0.086†	0.311 ± 0.131	0.714 ± 0.413
	0.102 ± 0.033	0.141 ± 0.048	0.227 ± 0.083	0.319 ± 0.133	0.636 ± 0.139
MI with VA	0.128 ± 0.255	0.176 ± 0.064	0.281 ± 0.116	0.367 ± 0.125	0.663 ± 0.147
	0.103 ± 0.044	0.128 ± 0.050‡	0.223 ± 0.114	0.305 ± 0.135	0.650 ± 0.188

**P* < .05 false-negative VLP vs normal subjects. †*P* < .05 false-negative vs true-negative VLP. ‡*P* < .05 false-negative vs true-positive VLP. FN = false negative; FP = false positive; MI = myocardial infarction; TN = true negative; TP = true positive; VA = ventricular arrhythmias; VLP = ventricular late potential.

Figure 3 Scatter plot out b/a ratio in each of 4 high-frequency bands. Brown * marks in the graphs indicate b/a ratios (300, 250, 200, 150 Hz) of post-myocardial infarction patients with lethal ventricular arrhythmias, and blue + marks b/a ratios of post-myocardial infarction patients without lethal ventricular arrhythmias. The dotted lines show the cut-off values of b/a ratios obtained from receiver-operator characteristic curves. L-VA(-) = myocardial infarction without lethal ventricular arrhythmias; L-VA(+) = myocardial infarction with lethal ventricular arrhythmias; N = normal group.



true-negative VLP group ($P < .05$). In addition, there was a difference in the b/a ratio between false-negative and true-negative VLPs groups at 250 Hz. But no significant differences among groups were found at 100 Hz.

In the present study, the cut-off values of the b/a ratios were decided for the parameters of ROC curves. Figure 3 shows the scatter plots of b/a ratios from post-MI patients with and without L-VAs. The transverse scales indicate b/a ratios from normal subjects. The numbers enclosed by squares along the dotted line in each panel indicate the optimum cut-off values of b/a ratios calculated from ROC curves. If the b/a ratios deviated from these values, the IQHFP was considered the abnormal signal. The statistical predictive values of L-VAs with MI are summarized in Table 3. As shown in the table, the specificity (93.8%) was characteristically higher at 300 Hz, although the sensitivity was lower. The sensitivity of L-VAs measured from VLPs was 53.3% in this study, but the negative predictive value was 74.7%. When the occurrence of

L-VAs was predicted using positive VLPs plus 1 or more abnormal IQHFPs that appeared at high-frequency bands (200, 250, or 300 Hz), 14 of 21 false-negative VLPs became positive cases. Consequently, the sensitivity of L-VAs predicted from both VLPs and b/a ratios (P300, P250, and P200/P80) increased from 53.3% to 89.5%, and its negative predictive value from 74.6% to 87.7%.

Q-S_p time and duration of IQHFP in each frequency band

The Q-S_p times in normal subjects ranged from 35 to 40 ms, in which the peak power of IQHFP appeared at the descending limb of the QRS complex in precordial chest leads, and appeared near the peak of the R wave in lead II. The Q-S_p time was changed, depending on the ECG lead. The Q-S_p times were measured from the QRS complexes in lead V₁ or V₂ in half of the normal subjects and from the QRS complexes in lead II in the remaining normal subjects. The average Q-S_p time was 34.3 ± 6.2 ms ($n = 37$) in normal subjects. The Q-S_p times in post-MI patients with L-VAs were significantly longer at only 300 Hz (45.7 ± 17.1 ms, $n = 45$) than in those without L-VAs (35.8 ± 11.5 ms, $n = 97$).

An example of changes in Q-S_p time during the clinical course is presented in Figure 4. The patient was a 52-year-old man who presented at the emergency department complaining of chest pain. The emergent coronary angiogram showed total occlusion of the proximal left anterior descending artery (segment 6). After coronary stenting, the patient’s ECG revealed a typical anterior MI. On the 2nd day of admission, while in the coronary care unit, he suffered a spontaneous incident of sustained ventricular tachycardia. Seven days after admission, his VLPs were positive and Q-S_p time was 55.5 ms as shown

Table 3 Predictive values of lethal ventricular arrhythmias measured from patients with myocardial infarction

b/a ratio or/ and VLP	Sensitivity (%)	Specificity (%)	PPV (%)	NPV (%)
P300/P80	27.9	93.8	66.7	74.6
P250/P80	37.2	79.4	44.4	74.0
P200/P80	25.5	87.6	47.8	72.6
P150/P80	23.2	85.6	41.6	71.5
VLP	53.3	63.9	40.7	74.7
VLP plus P300, 250, 200/ P80	89.5	63.3	67.4	87.7

PPV = positive predictive value; NPV = negative predictive value; VLP = ventricular late potential.

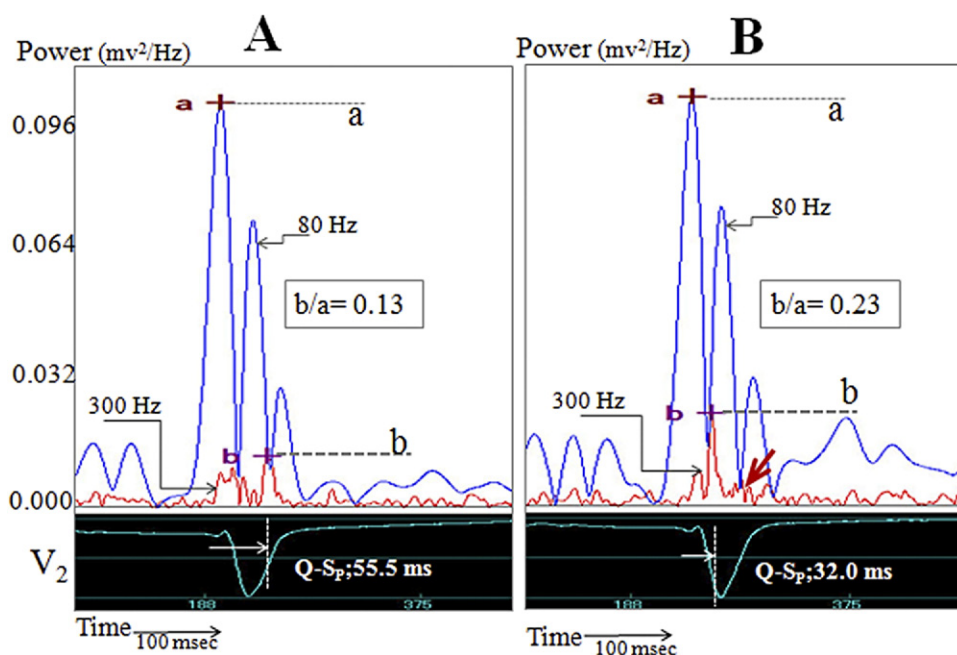


Figure 4 An example of changes in appearance time of the peak frequency power at 300 Hz. The blue lines indicate WT-ECG signals at 80 Hz. The red lines indicate WT-ECG signals at 300 Hz. **a** and **b** indicate the peak frequency power of WT-ECG signal at 80 Hz or 300 Hz within the QRS complex, respectively. WT-ECG signals are shown 7 days after admission in **A**, and after 10 days in **B**. $Q-S_p$ = appearance time of the peak wavelet signal from the onset of the QRS complex at 300 Hz; WT-ECG = wavelet-transformed electrocardiogram.

in Figure 4A. However, his VLPs changed from positive to negative after 10 days, and the b/a ratio increased from 0.13 to 0.23, which was clearly an abnormal value of IQHFP as shown in Figure 4B. At the same time, the $Q-S_p$ time was shortened from 55.5 to 32.0 ms, because the IQHFP located at the terminal phase of the QRS complex was reduced, as shown in Figure 4B and indicated by the red arrow.

Beat-to-beat variation of IQHFP

To assess the beat-to-beat variation of IQHFP, 10 patients with typical abnormal IQHFP were selected from all patients with MI. The percentage changes in the peak power of IQHFP and coefficient of variance were calculated from 10 consecutive QRS complexes in the chest lead (V_1 or V_2). Mean percentage changes and coefficients of variance were $29.2\% \pm 26.9\%$ and 0.96 at 300 Hz, $25.1\% \pm 18.8\%$ and 0.75 at 200 Hz, $17.6\% \pm 12.2\%$ and 0.70 at 100 Hz. Thus, a frequency dependent decrease in the variation of WT-ECG signals was observed. From these results, the maximum b/a ratio was selected from the values during a single respiratory cycle (about 3 to 6 beats).

Discussion

The key results obtained in this study were as follows: (1) A single-beat analysis using CWT was successfully used to search IQHFP. (2) The combined use of VLPs and IQHFP improved the sensitivity of VLPs for prediction of L-VAs in post-MI patients from 53.3% to 89.5%, and the negative predictive value from 74.7% to 87.7%. (3) The $Q-S_p$ times in post-MI patients with L-VAs were found to be significantly longer at only 300 Hz (45.7 ± 17.1 ms) than in those without L-VAs (35.8 ± 11.5 ms).

High-frequency powers within the QRS complex and use of the b/a ratio

In the early 1950s, Langner et al¹⁴ were first to appreciate that high-frequency notches and slurs in the QRS complex appeared more frequently in patients with MI. Subsequently, the investigators referred to the notching and slurring of the expanded QRS as high-frequency components in post-MI patients.^{15,16} Since the 1980s, SAECG has been used to reduce the noise and to search for abnormal high-frequency potentials. However, there are some weaknesses in VLP assessment at abnormal high-frequency potentials within the QRS complex. First, the cardiac excitation fronts passing through the anterior region of the left ventricle originate in the early phase of the QRS complex. Delayed abnormal depolarization potentials of these regions may not outlast the QRS complex. Secondly, high-frequency potentials within the QRS complex might eventually be smoothed by poor alignment of QRS complexes. Therefore, the single-beat analysis used in the present study provides different raw information of high-frequency signals hidden within the QRS complex. As shown in Figure 1, if 2 WT-ECG signals at low- and high-frequency bands were selected, the intra-QRS signal with high-frequency band (300 Hz) was easily discriminated from the signals that appeared at time sections other than the QRS complex. Previous studies also showed that good time-frequency resolution in analyzing a single beat was obtained without signal averaging.^{13,17,18} Quantitative assessment at a power ratio such as the b/a ratio is proper for comparison with the power values of WT-ECG signals among individuals, because the power ratio can diminish variations among individuals and from beat to beat.

Time and frequency domain analysis of QRS complex

A number of studies have reported noninvasive assessment of prediction of L-VAs using time or/and frequency domains.^{2,4,9–10} For example, Kelen et al^{9,19} used spectral turbulence analysis of the SAECG as a method to analyze frequency domain, and this method has been used to date. In their method, based on the short-time Fourier transform, the total predictive accuracy for L-VAs inducibility was improved from 73% of VLPs to 94% of spectral turbulence analysis. Others introduced the wavelet correlation function, which combines wavelet transform with a modified analysis of spectral turbulence, because wavelet transform yields a better time-frequency resolution than short-time Fourier transform. The combined application of the wavelet transform correlated function of the SAECG and VLPs for prediction of L-VAs increased the total predictive accuracy up to 20% to 25%.^{11,20} However, the location of the abnormal signal during the QRS complex was uncertain in these studies. Couderc et al¹¹ demonstrated that the most significant wavelets, ranging from 125 to 250 Hz, were localized around the terminal portion of the signal-averaged QRS complex. In contrast, in the present study, the abnormal IQHFP was found in the QRS complex; namely the longest average Q-S_p time among high-frequency bands was 45.7 ms. This different result may be ascribed to differences in the analytical methods between SAECG and a single QRS complex. It is conceivable that the transient high-frequency potentials hidden in the QRS complex that occurred at the early to terminal portion were smoothed by signal averaging. On other hand, the VLPs with very low amplitude could not be captured by single-beat analysis in the present study. If these considerations are sound, the combined use of VLP and IQHFP for the prediction of L-VAs in post-MI patients is more accurate compared with the methods of previous studies.

Study limitations

The elimination of noises and baseline drift are needed to perform CWT analysis with a single QRS complex. Another limitation for the application of the CWT method was finding abnormal IQHFP in <2% of normal subjects; therefore, the CWT method was less effective than the VLP method in discriminating normal subjects from post-MI patients with L-VAs.

Conclusions

The study demonstrated that the combined use of VLPs and IQHFP improved the sensitivity of VLPs for prediction of L-VAs in post-MI patients from 53.3% to 89.5%, and the negative predictive value from 74.7% to 87.7%. The improvement was chiefly attributed to the recognition of abnormal IQHFP in a high percentage (67%) of post-MI patients judged on false-negative VLPs. The measurements of the appearance time of IQHFP can play a role in subsidiary understanding of the pathogenesis of L-VAs.

Acknowledgements

The authors acknowledge Professors Ryuichi Ashino, Takeshi Mandai, and Akira Morimoto, who comprise the activity group on wavelet analysis affiliated with the Japanese Society for Industrial and Applied Mathematics. They provided appropriate advice on the application of wavelet function and the theoretical background for the present study.

References

1. Rubart M, Zipes DP. Mechanisms of sudden cardiac death. *J Clin Invest* 2005;115:2305–2315.
2. Simson MB, Untereker WJ, Spielman SR, et al. Relation between late potentials on the body surface and directly recorded fragmented electrograms in patients with ventricular tachycardia. *Am J Cardiol* 1983;51:105–112.
3. Santangeli P, Infusino F, Sgueglia GA, Sestito A, Lanza GA. Ventricular late potentials: a critical overview and current applications. *J Electrocardiol* 2008; 41:318–324.
4. Lander P, Gomis P, Goyal R, et al. Analysis of abnormal intra-QRS potentials. *Circulation* 1977;95:1386–1393.
5. Das MK, Zipes DP. Fragmented QRS: A predictor of mortality and sudden cardiac death. *Heart Rhythm* 2009;6:S8–S14.
6. Lanza GA. The electrocardiogram as a prognostic tool for predicting major cardiac events. *Prog Cardiovasc Dis* 2007;50:87–111.
7. Bauer A, Guzik P, Barthel P, et al. Reduced prognostic power of ventricular late potentials in post-infarction patients of the reperfusion era. *Eur Heart J* 2005; 26:755–761.
8. Boineau JP, Cox JL. Slow ventricular activation in acute myocardial infarction: A source of re-entrant premature ventricular contractions. *Circulation* 1973;48: 702–713.
9. Kelen GJ, Henkin R, Starr A-M, Caref EB, Bloomfield D, El-Sherif N. Spectral turbulence analysis of the signal-averaged electrocardiogram and its predictive accuracy for inducible sustained monomorphic ventricular tachycardia. *Am J Cardiol* 1991;67:965–975.
10. Haberl R, Jilge G, Pulter R, Steinbeck G. Spectral mapping of the electrocardiogram with Fourier transform for identification of patients with sustained ventricular tachycardia and coronary artery disease. *Eur Heart J* 1989;10: 316–322.
11. Couderc J-P, Chevalier P, Fayn J, Rubel P, Touboul P. Identification of post-myocardial infarction patients prone to ventricular tachycardia using time-frequency analysis of QRS and ST segments. *Europace* 2000;2:141–153.
12. Morlet D, Peyrin F, Desseigne P, Touboul P, Rubel P. Wavelet analysis of high-resolution signal-averaged ECGs in postinfarction patients. *J Electrocardiol* 1993;26:311–320.
13. Gramatikov B, Brinker J, Yi-Chun S, Thakor NV. Wavelet analysis and time-frequency distributions of the body surface ECG before and after angioplasty. *Comput Methods Programs Biomed* 2000;62:87–98.
14. Langner PH Jr. Further studies in high fidelity electrocardiography: myocardial infarction. *Circulation* 1953;8:905–913.
15. Langner PH Jr, Geselowits DB, Mansure FT. High-frequency components in the electrocardiograms of normal subjects and of patients with coronary heart disease. *Am Heart J* 1961;62:746–755.
16. Flowers NC, Horan LG, Tolleson WJ, Thomas JR. Localization of the site of myocardial scarring in man by high-frequency components. *Circulation* 1969; 40:927–934.
17. Takayama H, Yodogawa K, Katoh T, Takano T. Evaluation of arrhythmogenic substrate in patients with hypertrophic cardiomyopathy using wavelet transform analysis. *Circ J* 2006;70:69–74.
18. Popescu M, Laskaris N, Chilandakis I, et al. Beat-to-beat wavelet variance of the QRS complex as a marker of arrhythmogenic substrate in ventricular tachycardia patients. *Physiol Meas* 1998;19:77–92.
19. Bechimol-Barbosa PR, Nasario-Junior O, Nadal J. The effect of configuration parameters of time-frequency maps in the detection of intra-QRS electrical transients of the signal-averaged electrocardiogram: Impact in clinical diagnostic performance. *Int J Cardiol* 2010;145(1):59–61.
20. Reinhardt L, Mäkijärvi M, Fetsch T, et al. Predictive value of wavelet correlation functions of signal-averaged electrocardiogram in patients after anterior versus inferior myocardial infarction. *J Am Coll Cardiol* 1996;27:53–59.